ACS APPLIED MATERIALS & INTERFACES

Research Article

www.acsami.org

In Situ Method for Measuring the Mechanical Properties of Nafion Thin Films during Hydration Cycles

Kirt A. Page,[†] Jae Wook Shin,[†] Scott A. Eastman,[‡] Brandon W. Rowe,[†] Sangcheol Kim,[†] Ahmet Kusoglu,[§] Kevin G. Yager,[∥] and Gery R. Stafford*[,†]

[†]Materials Science and Engineering Division, National Institute of Standards and Technology, Gaithersburg, Maryland 20899, United States

[‡]United Technologies Research Center, East Hartford, Connecticut 06108, United States

[§]Energy Storage and Distributed Resources Division, Lawrence Berkeley National Laboratory, Berkeley, California 94720, United States

[∥]Center for Functional Nanomaterials, Brookhaven National Laboratory, Upton, New York 11973, United States

Supporting Information

ABSTRACT: Perfluorinated ionomers, in particular Nafion, are an essential component in hydrogen fuel cells, as both the proton exchange membrane and the binder within the catalyst layer. During normal operation of a hydrogen fuel cell, the ionomer will progressively swell and deswell in response to the changes in hydration, resulting in mechanical fatigue and ultimately failure over time. In this study, we have developed and implemented a cantilever bending technique in order to investigate the swelling-induced stresses in biaxially constrained Nafion thin films. When the deflection of a cantilever beam coated with a polymer film is monitored as it is exposed to varying humidity environments, the swelling induced stress-thickness product of the polymer film is measured. By combining the stress-thickness results with a measurement of the swelling strain as a function of humidity, as measured by quartz crystal microbalance (QCM) and X-ray reflectivity (XR), the swelling stress can be determined. An estimate of the Young's modulus of thin Nafion films as a function of relative humidity is obtained. The Young's modulus values indicate orientation of the ionic domains within the polymer films, which were confirmed by grazing incidence small-angle X-ray scattering (GISAXS). This study represents a measurement platform that can be expanded to incorporate novel ionomer systems and fuel cell components to mimic the stress state of a working hydrogen fuel cell.

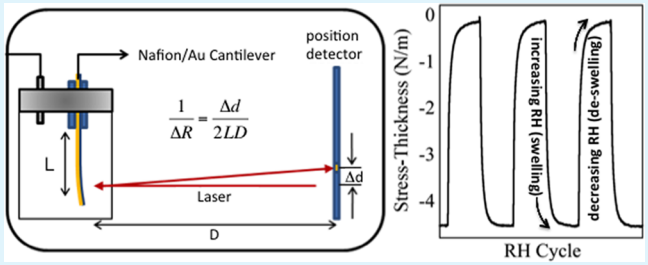

KEYWORDS: *stress, thin films, Nafion, curvature, modulus, humidity*

INTRODUCTION

Perfluorosulfonic acid (PFSA) ionomers are the most widely studied class of materials to be used as proton exchange membranes in fuel cell applications due to their excellent properties including, but not limited to, (1) high proton conductivity, (2) negligible electrical conductivity, (3) selective permeability to ions, (4) resistance to permeation of uncharged gases, (5) chemical stability, and (6) good mechanical strength. Nafion, the most commonly studied PFSA, consists of a perfluoroethylene backbone with flexible perfluorinated vinyl ether side chains terminated by a sulfonic acid group as shown below.

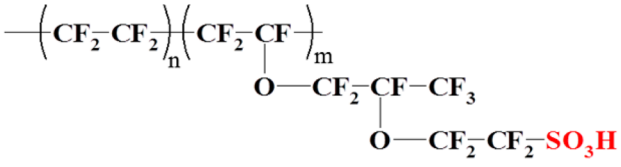

The perfluoroether side chains, bearing a terminal, sulfonate functionality, have been shown to aggregate, thus leading to a nanophase separated morphology composed of hydrophilic ionic clusters distributed throughout a continuous, hydrophobic semicrystalline polytetrafluoroethylene matrix.[1] It is this phase separated morphology that is, in part, responsible for the performance of these materials in a working fuel cell and similar electrochemical energy conversion devices. However, in an operating fuel cell, the cycles of hydration and dehydration, and the mechanical response thereto, threaten the long-term mechanical stability of the membrane and, thus, performance and device lifetime. Therefore, it is critical that one have an understanding of the water-dependent mechanical response and properties of PFSA membranes.

When fully hydrated, a typical perfluorosulfonic acid (PFSA) proton exchange membrane is known to swell by 20% in all directions.[2] However, the membranes are biaxially constrained in a fuel cell, and significant stresses develop during swelling.

Received: May 20, 2015
Accepted: July 30, 2015
Published: August 10, 2015

DOI: 10.1021/acsami.5b04080
ACS Appl. Mater. Interfaces 2015, 7, 17874−17883

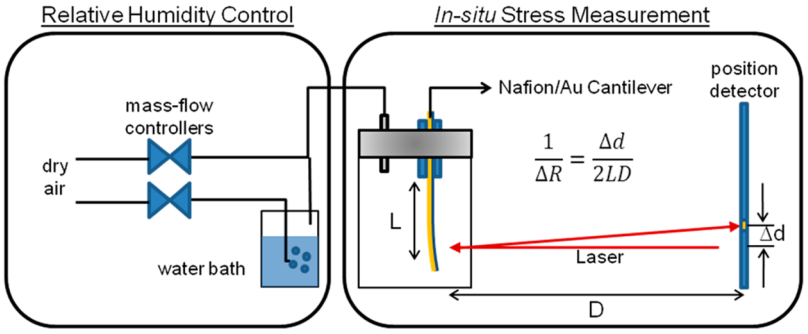

Figure 1. Schematic of relative humidity control system and in situ cantilever curvature measurement system.

Membrane failures have been brought about by cycling between wet and dry operating conditions, without the passage of current or the presence of reactants/products.[3,4] These hydration cycles expose the membrane to both tensile and compressive stress, causing buckling, delamination, and/or tearing. In order to improve membrane durability and service life, a better understanding of failure modes and possible mitigation strategies is required.

Nafion is a viscoelastic material that responds dramatically to changes in hydration and stress. Water absorption increases the volume of Nafion by an amount of $\Delta V/V_o = ((1 + \varepsilon_w)^3 - 1)$ where V_o is the initial volume of dry membrane and ε_w is the linear swelling expansion due to the absorption of water.[5] For a free-standing membrane equilibrated in liquid water, ε_w is approximately 0.2, which corresponds to a 72% volume expansion.[2] The expansion of a fully constrained membrane, as is the case in a working fuel cell, generates strain (deformation) energy as the membrane attempts to swell from water absorption. The corresponding stress often exceeds the yield stress, thus giving rise to irreversible plastic deformation that leads to structural degradation. Many recent studies have focused on developing analytical and numerical models to capture the hygrothermal stress behavior as a result of humidity cycling. A variety of constitutive frameworks have been employed, including linear elasticity,[6,7] elastic-plasticity,[8−11] viscoelasticity,[3,4] and viscoplasticity.[12−15] Evidence of strain hardening has also been reported.[2,16,17]

Clearly, the literature demonstrates that there is extensive understanding of the mechanical response of *bulk* membranes to hygro-thermal stresses. More recently, there has been an increased interest in the material properties of PFSAs under thin film confinement. This interest stems from the fact that in the catalyst layer, where the PFSA is used as a binder, the polyelectrolyte is heterogeneously dispersed and can be confined to films as thin as tens of nanometers among the nanoparticulate platinum and the carbon support. Recent studies have demonstrated that under confinement these materials can show marked changes in properties such as water uptake and transport, which are critical to material performance in a working fuel cell.[18−28] Studies in this field are ongoing, and there is still much to learn about material properties under confinement and the molecular and nanoscale structural origins for the observed deviations from bulk membrane properties. Despite the importance of the mechanical response of membranes to hydration cycles, which is critical to lifetime and durability of PFSA as a solid-electrolyte but also as a thin film in fuel cell catalyst layers, there has been no effort to study these behaviors in thin films. This is largely due to the lack of measurement techniques and platforms capable of measuring the mechanical properties of PFSA films that are only tens of nanometers thick. Page et al.[28] recently demonstrated a confinement-driven increase in the modulus of Nafion thin films using a buckling methodology under ambient conditions. However, there is a need for more comprehensive measurement techniques for studying the deformation of PFSA thin films especially during humidity changes. In this work, we present measurements based on a cantilever curvature method which has proven to be an excellent method for replicating and measuring the stresses that develop in thin film materials. We have successfully applied this technique to a PFSA thin film in response to humidity cycling and demonstrate its efficacy in determining and understanding the mechanical properties. While this paper is focused more on the development and validation, through the use of quartz crystal microbalance (QCM), X-ray reflectivity (XR), and grazing incidence small-angle X-ray scattering (GISAXS), of the cantilever curvature measurement, future studies will apply this technique to a range of film thicknesses and environmental conditions in order to gain a more fundamental understanding of the behavior of PFSAs under thin film confinement. Not only does this measurement platform provide the opportunity to study the in situ mechanical response of Nafion thin films, but it can be applied to novel membrane materials and PEM fuel cell components in a way that allows for easy evaluation of the mechanical response under conditions that mimic the biaxial stresses present in a working PEM fuel cell.

EXPERIMENTAL SECTION

Cantilever Curvature Measurements. The change in stress of a Nafion film was measured as a function of relative humidity (RH) using in situ wafer curvature. A schematic of the humidity control system and in situ cantilever curvature measurement system is shown in Figure 1. The substrate was a borosilicate glass cantilever (Schott North America, Inc.) with dimensions of 60 mm × 3 mm × 108 μm, that had been coated on one side with 5 nm of Ti followed by 250 nm of Au by electron beam evaporation. The glass cantilever had a Young's modulus of 72.9×10^9 N/m^2 and a Poisson's ratio of 0.208.

Nafion dispersions of 1100 equiv molecular mass, dissolved 20% by mass in a mixture of lower aliphatic alcohols and water, containing 34% by mass water (Sigma-Aldrich) were diluted in anhydrous ethanol at a ratio of 1:4 by volume. The Nafion dispersion was used to deposit a thin film on the Au surface using an established flow coating technique.[29] The thickness of the Nafion film was determined to be 216 ± 34 nm via ellipsometry. The relatively large variation in film thickness was determined to be caused by edge effects during the flow-coating process. The Nafion film was annealed at 60 °C for 2 h.

The Nafion-coated cantilever was mounted in a 25 mL Pyrex cell. A glass disk was joined to the back of the cell to allow it to be held and positioned by a standard mirror mount on the optical bench. The cell was equipped with an air flow inlet tube, and a small hole in the top of

DOI: 10.1021/acsami.5b04080
ACS Appl. Mater. Interfaces 2015, 7, 17874−17883

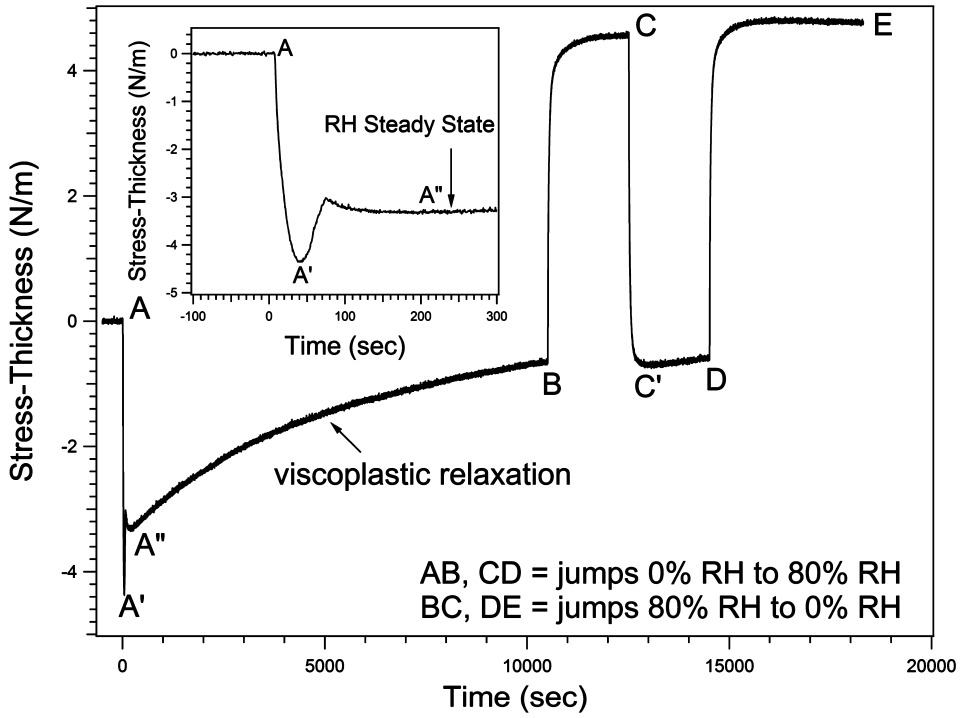

Figure 2. Change in stress-thickness during relative humidity jumps between 0% and 80% RH. AB and CD represent humidity jumps from 0% to 80% RH while BC and DE represent humidity jumps from 80% to 0% RH. The inset is the magnification of the spike observed during the first water uptake.

the cell served as the gas exit. The RH in the cell was controlled by mixing dry and humidified air. The humidified air was generated by flowing dry air from a gas cylinder through a deionized water reservoir. Two mass flow controllers (MKS type 146C) were connected in parallel and programmed to deliver a total flow rate of 500 ± 5 mL/min. Controller A metered the flow rate of dry air (0% RH) while controller B metered the flow rate of humidified air. The vapor pressure of water within the cell was adjusted by tuning the flow ratio of each controller, keeping the total flow rate at 500 ± 5 mL/min. The actual RH value was calibrated using a humidity/temperature controller (ETS-5200-240-230). The measured RH reached a steady state value in 2 to 3 min and deviated from the nominal value that was calculated from the ratio of the gas mixture (shown in Figure S1). The measured RH value was only 82(±2)% when the nominal RH was set to 100%.

The curvature of the substrate was monitored by reflecting a HeNe laser off of the glass/metal interface (Nafion-free side) onto a position-sensitive detector. The relationship between the force per cantilever beam width (ΔF_c) exerted by the Nafion film and the radius of curvature of the cantilever is given by Stoney's equation.[30]

$$\Delta F_c = \frac{E_s h_s^2}{6(1-\nu_s)\Delta R} = \sigma_{Bi} h_f \quad (1)$$

where E_s, ν_s, and h_s are the Young's modulus, Poisson's ratio, and thickness of the glass substrate, respectively. A single stationary laser measures only the change in curvature, rather than absolute curvature, by measuring the deflection. As a consequence, ΔF_c is arbitrarily set to zero at the beginning of the experiment or measurement. The measured cantilever force (ΔF_c) is equal to the average biaxial stress of the Nafion film (σ_{Bi}) multiplied by its thickness (h_f). Throughout this paper, ΔF_c will be referred to as the stress-thickness. Since the thickness of the Nafion is less than 1% that of the glass substrate, we use the thin film form of Stoney's equation as shown in eq 1. This simplification introduces an error of less than 1%. This system can resolved changes in stress-thickness down to about 0.01 N/m. Details of the experimental apparatus and procedures for the stress measurement are described elsewhere.[31,32]

X-ray Reflectivity (XR). A Philips X'pert X-ray diffractometer was used to characterize the equilibrium film thickness and water content of Nafion thin films exposed to a series of water vapor concentrations. Reflectivity data were collected in the specular condition with the grazing incident angle equal to the detector angle. The incident angle was adjusted from 0.1° to 1.0° with a step size of 0.0003°. The voltage and current of the X-ray source were set to 45 kV and 40 mA, respectively. The instrument was equipped with a temperature controlled environmental chamber fitted with beryllium windows, a humidified air inlet, and an exhaust port with a humidity sensor. The vapor pressure of water within the sample chamber was controlled via the same external mass flow device as described above for the cantilever curvature method; however, the equilibration times were much longer due to the larger sample environment. The humidity in the chamber was monitored in situ via a temperature/humidity sensor with a precision of ±2% RH and ±0.5 °C, and it took approximately (20 to 30) min for the system to equilibrate after a change in the humidity set point. All measurements were done at ambient temperature (27 °C ± 0.5 °C).

Nafion dispersions of 1100 equiv molecular mass, dissolved 20% by mass in a mixture of lower aliphatic alcohols and water, containing 34% by mass water (Sigma-Aldrich) were diluted in anhydrous ethanol at a ratio of 1:4 by volume and spun onto gold-coated silicon wafers at 2000 rpm for 1 min. The Nafion thin film/wafer assembly was mounted onto the stage and enclosed with the X-ray transparent encasement. After mounting, the Nafion film was dried under a continuous flow (500 mL/min) of dry air overnight at room temperature. The thickness, scattering length density, and surface roughness were determined by modeling based on the Parratt formalism,[33] and the "reflpak" software was used to fit the data. Reflectivity data acquired immediately after drying were used to determine the initial, dry film thickness for each film. Films were then subjected to a series of increasing relative humidity ranging from 0% to 75% RH at 27 °C ± 0.5 °C. The sample was allowed to equilibrate for 1 h at each RH before collecting the XR data. The sample equilibration time was determined from monitoring the critical edge and the first two interference fringes in the reflectivity data. After 1 h, no appreciable change in either the critical angle or the first two fringes

DOI: 10.1021/acsami.5b04080
ACS Appl. Mater. Interfaces 2015, 7, 17874−17883

was observed, implying that the samples had equilibrated with respect to absorbed water and film swelling. Note that the sample equilibrated slower than the time for the humidity in the chamber to change.

Grazing Incidence Small-Angle X-ray Scattering (GISAXS). GISAXS experiments were performed at the X9 undulator-based beamline at the National Synchrotron Light Source. An incident X-ray beam of energy 13.5 keV (wavelength = 0.0918 nm) was collimated using a two-slit system and focused to a beam 100 μm wide by 60 μm tall at the sample position using a Kirkpatrick-Biaz mirror system. Samples were mounted inside a small humidity-controlled chamber with Kapton windows.

Grazing-incidence experiments were performed over a range of incidence angles, both below and above the film-vacuum critical angle. Two-dimensional scattering images were collected using a charge-coupled device (CCD) detector. Data conversion of images to q-space was accomplished after calibration using silver behenate powder as a standard.

Quartz Crystal Microbalance (QCM). Gold coated AT-cut, 14 mm diameter, 4.95 MHz quartz crystals were purchased from Q-Sense (Sweden). Measurements were conducted using a Q-Sense E4, which has a variable data acquisition rate and a maximum mass sensitivity of 0.5 ng/cm^2. Humidity in the QCM sample chamber was controlled using a mass flow control system similar to the one described in the cantilever curvature experiments. Thin films were prepared by spin coating directly on the Q-Sense crystals following the same procedure used for XR sample preparation. Films were stored under ambient conditions until measurement, typically less than 24 h. The initial dry mass of Nafion was determined by allowing the film to equilibrate under dry nitrogen until the resonance frequency was stable. Water mass sorption was determined at various relative humidity levels by relating changes in the resonance frequency to mass uptake using the Sauerbrey equation.

$$\Delta f = -\frac{2f_o^2}{A\rho_q v_q}\Delta m \tag{2}$$

where Δf is the frequency change, f_0 is the resonance frequency, Δm is the mass change, A is the piezoelectrically active crystal area, ρ_q is the quartz density, and v_q is the transverse wave velocity in quartz.

RESULTS AND DISCUSSION

Stress Relaxation and Initial Hydration. Figure 2 is a plot of the stress-thickness response of the Nafion thin film on the Au-coated cantilever. Initially, dry air was passed through the cell for about 500 s in order to obtain a stable reference stress at 0% RH. During the periods AB and CD, the RH was maintained at 80% while during the periods BC and DE, the RH was maintained at 0%. During the initial humidity jump (AB), the Nafion film stress increased in the compressive direction due to volume swelling; however, most of the compressive stress relaxed within about 3 h. When the water was removed from the Nafion film during the 0% RH cycle (BC), the elastic strain in addition to the plastic strain, that developed during the visco-plastic relaxation in period AB, resulted in a net tensile stress. During this dehydration cycle (BC) and the following cycles (CD and DE), little stress relaxation was observed and the magnitude of stress-thickness change was essentially the same (≈5.3 N/m), indicating primarily elastic behavior during hydration cycles. The inset of Figure 2 shows the stress relaxation during the first water uptake in more detail. At point A, the stress-thickness began to increase (compressively) in response to the 80% RH. However, the stress-thickness reached a maximum point (A') at 40 s and decreased rapidly until it began increasing again at about 70 s. At about 200 s, the stress-thickness shows a second peak (A'') followed by stress relaxation with a much slower rate of decay. As mentioned previously, the RH of the cell reached steady state in about 3 min after the RH was increased from 0% to 80%. This indicates that the stress changes that occur in the first few minutes of the initial hydration take place well before the RH reaches 80%.

Figure 2 indicates that the structural changes associated with the visco-plastic relaxation are essentially complete after about a 3 h exposure to 80% RH and that subsequent hydration cycles show primarily elastic behavior. Although some relaxation is still readily apparent during the hydration cycle (C′D in Figure 2), the response over a hydration cycle is generally elastic. This elastic behavior, and its stability over time, is clearly shown in the additional hydration cycles shown in Figure 3. The 50 cycles shown in Figure 3a reveal steady state elastic behavior over the nearly 14 h duration of the experiment. Each hydration cycle produces a stress-thickness change of approximately −4.4

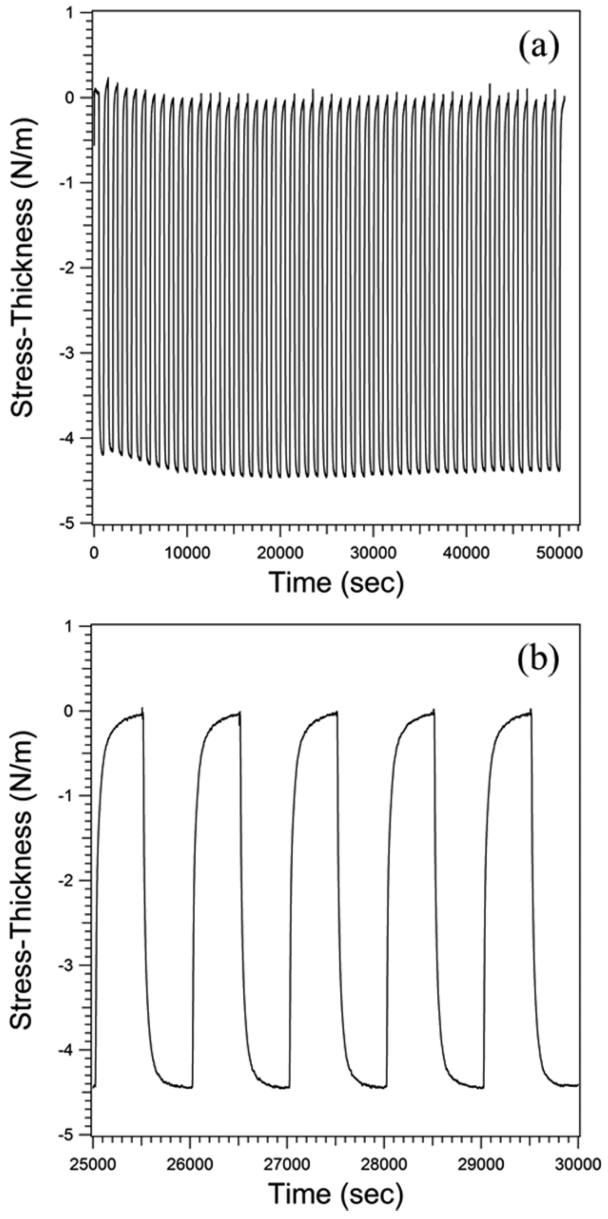

Figure 3. (a) Change in stress-thickness during relative humidity cycling following the initial hydration cycle shown in Figure 2. The relative humidity was cycled between 0% and 80% at 500 s intervals for a total of 50 cycles; (b) 5 cycles magnified from (a).

DOI: 10.1021/acsami.5b04080
ACS Appl. Mater. Interfaces 2015, 7, 17874−17883

N/m. The fact that the cantilever returns to its original position following the 50 cycles confirms that the Nafion responds elastically to the changes in humidity.

Figure 3b shows a magnified view of 5 of the hydration cycles. The stress response of the hydration and dehydration cycles has a similar shape, reaching 95% of the total stress change in the first 3 min. This is consistent with the time required for the humidity of the cell to reach steady state. These data indicate that, once the Nafion undergoes an initial break-in period, it responds elastically to changes in humidity.

Stress in Nafion Film as a Function of RH. The change in stress-thickness was measured while the RH was increased by 1% between 0% and 5% RH and by 5% between 5% and 80% RH. Each RH step was maintained for 1000 s. The RH was changed in two different ways, stepwise and pulsewise, as shown in Figure 4a,b, in order to determine if the steady state values of stress-thickness are path-independent. When the RH was increased, the stress-thickness changed rapidly and steady state was reached in about 1 to 2 min for the stepwise case and about 2 to 3 min for the pulsewise case. As stated previously, this is roughly the time required for the measured RH in the cell to reach a steady state value.

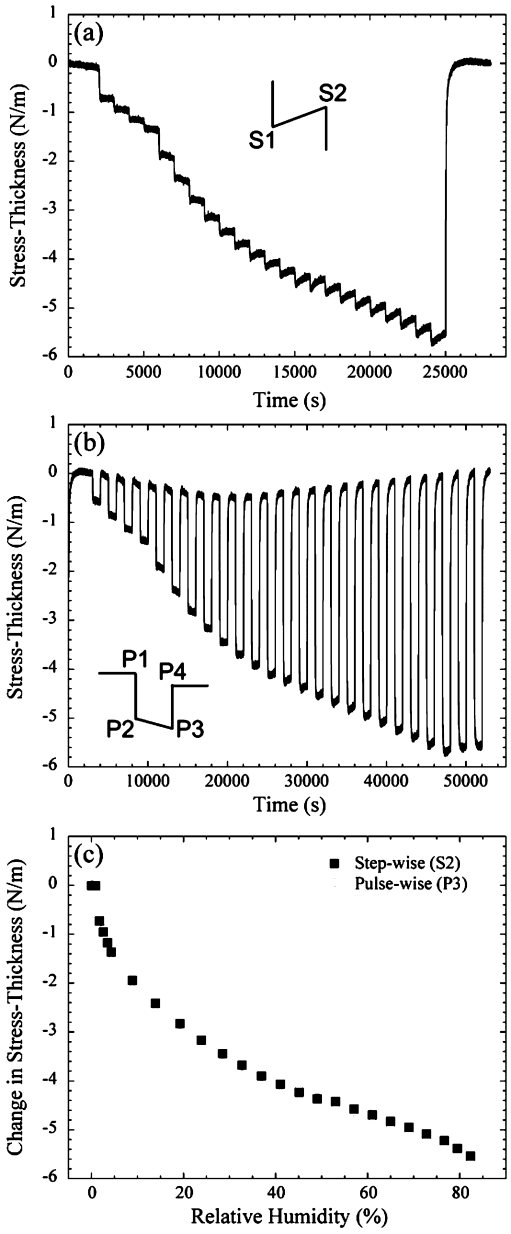

Figure 4. Plot of stress-thickness vs time as RH is increased, (a) stepwise and (b) pulsewise. (c) The plot of stress-thickness vs RH for the stepwise data taken at S2 and the pulsewise data taken at P3.

After the steep initial stress-thickness change in the compressive direction, the stress-thickness changes slowly in a direction that appears to depend on the RH value. This response was observed for both the stepwise and pulsewise measurements. Viscoplastic stress relaxation, like that observed during the initial hydration cycle, can be ruled out since the stress-thickness generally returned to its initial value of 0 N/m when the film returned to the dry state at the end of the experiment. However, the pulsewise experiment in Figure 4b does show a baseline drift that is similar in both magnitude and direction to the apparent stress relaxation observed during the hydration pulse. Viscoelastic behavior has been observed in cantilever bending experiments involving a bilayer comprised of a 25 μm thick Nafion film constrained by a 250 μm thick PEEK (polyether ether ketone) substrate to which it was bonded.[34] This relaxation was attributed to the elastic properties of the Nafion adjusting to the change in RH rather than plastic yielding. As will be shown later, the elastic modulus of Nafion is known to decrease with increasing RH.[8,35,36] However, the baseline drift shown in Figure 4b prevents us at present from associating these stress changes with viscoelastic behavior.

The values of stress-thickness from both stepwise (S2) and pulsewise (P3) experiments, taken 1000 s after the RH change, are plotted as a function of RH in Figure 4c. The two values are almost identical, indicating that the steady state values of stress-thickness are path-independent and that any viscoelastic relaxation that may follow the RH change is a small part of the overall stress response. As expected, the general shape of the curve is very similar to water uptake isotherms that appear in the literature.[7,37]

Calculations of Mechanical Properties. If the Nafion film is assumed to be isotropic and not constrained by a substrate, water absorption increases its volume by $\Delta V/V_o = (1 + \varepsilon_w)^3 - 1$ where V_o is the initial volume of the dry membrane and ε_w is the swelling expansion of the film due to water absorption.[2,5,9,10] The stress-free strain in all directions are equal and, to first order, given by

$$\varepsilon_o = \left(\frac{V}{V_o}\right)^{1/3} - 1 \tag{3}$$

However, if the Nafion film is constrained to a substrate, biaxial elastic strain ($\varepsilon_E = \varepsilon_x = \varepsilon_y$) develops in the x- and y-directions and the total biaxial strain of the Nafion film is then the sum of the stress-free strain and the biaxial elastic strain.

$$\varepsilon_{tot} = \varepsilon_o + \varepsilon_E \tag{4}$$

The total biaxial strain of the Nafion film is assumed to be equal to that of the substrate since the Nafion thickness is less than 1% of the cantilever thickness and it is assumed that no delamination occurs between the Au and the Nafion. The total strain of the substrate surface can be calculated from the change in substrate curvature, where $\varepsilon_{tot} = -2/3\,(h_s/\Delta R)$.[38] The largest ΔR associated with the data in Figure 4 would give rise to a total strain of 2×10^{-6}. We can expect a biaxial elastic strain similar in magnitude to the reported 0.2 linear swelling expansion (ε_w) for a free-standing membrane equilibrated in

DOI: 10.1021/acsami.5b04080
ACS Appl. Mater. Interfaces 2015, 7, 17874−17883

liquid water.[5] As a consequence, with $\varepsilon_E \gg \varepsilon_{tot} \approx 0$, the biaxial elastic strain of the film is essentially equal to the stress free strain of the film in magnitude, but of opposite sign.

$$\varepsilon_E = -\varepsilon_o \tag{5}$$

The magnitude of the elastic strain of the film in the plane is proportional to the biaxial elastic stress (σ_{Bi}) of the film and given by

$$\varepsilon_E = \frac{1-\nu}{E}\sigma_{Bi} \tag{6}$$

where ν is Poisson's ratio and E is Young's modulus of the film. A strain in the z-direction (out of plane) will be generated by the biaxial elastic strain due to Poisson's effect

$$\Delta\varepsilon_z = -\frac{2\nu}{E}\sigma_{Bi} \tag{7}$$

Since the film is free to expand in the z-direction, the total strain in the thickness direction is the sum of the stress-free strain and Poisson's strain

$$\varepsilon_z = \varepsilon_o + \Delta\varepsilon_z \tag{8}$$

In order to calculate the average stress of the Nafion film, the variation of the thickness with water content needs to be considered. The thickness of the Nafion film is given by

$$h_f = (1+\varepsilon_z)h_o \tag{9}$$

where h_o is the thickness of the Nafion film when the film is fully dried. Recalling from eq 1 that

$$\Delta F_c = \sigma_{Bi}h_f \tag{10}$$

and substituting eqs 5−9 results in the following quadratic equations with respect to ε_o and ε_z, respectively.

$$\varepsilon_o^2 + \frac{1-\nu}{1+\nu}\varepsilon_o + \frac{(1-\nu)^2\Delta F_c}{(1+\nu)Eh_o} = 0 \tag{11}$$

$$\varepsilon_z^2 + \varepsilon_z + \frac{(1+\nu)\Delta F_c}{Eh_o} = 0 \tag{12}$$

Alternatively, one can rewrite the expression in terms of shear modulus, G, without using the Poisson's ratio in the expression

$$\nu = \frac{E}{2G} - 1 \quad \text{such that} \quad \varepsilon_z^2 + \varepsilon_z + \frac{1}{2G}\frac{\Delta F_c}{h_o} = 0 \tag{13}$$

Within eqs 11 and 12 are the values of the stress-thickness (ΔF_c), the stress free strain (ε_o), the total strain in the z-direction (ε_z), and the initial film thickness (h_o) which can all be measured or estimated from other measurement techniques such as wafer curvature, QCM, and XR, respectively. The only unknowns are the modulus and Poisson's ratio of the thin film.

It is well-known that the mechanical properties of Nafion vary with relative humidity. Therefore, it is necessary that we have reasonable estimates of how ΔF_c, ε_o, ν, and ε_z vary accordingly. The stress-free strain, ε_o, of the Nafion can be estimated/calculated using eq 3 as a function of relative humidity using the water uptake data (the values of which can be found in Figure S2) obtained from the QCM measurements, which are consistent with literature values reported for bulk Nafion,[39] and can be found in Figure 5. Our estimates for ε_o are in excellent agreement with those reported by Majsztrik et al. for Nafion 1100, obtained from water permeation data.[5] We

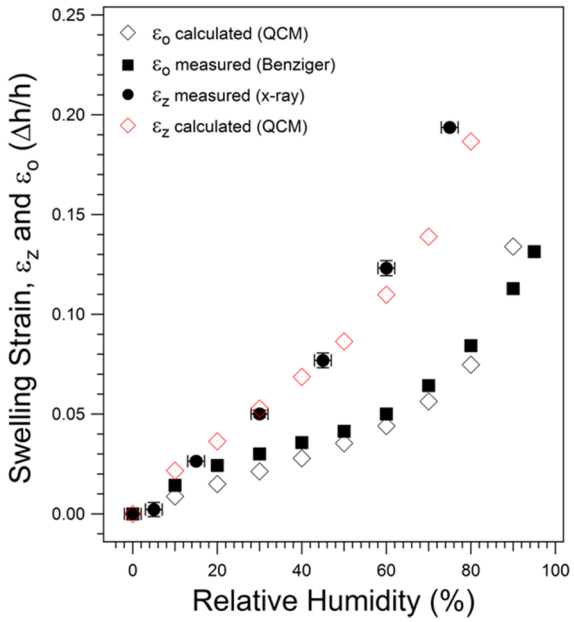

Figure 5. Plot of the stress free strain, ε_o, determined from the water uptake measurements and as measured by Benziger and co-workers[5] along with the swelling strain, ε_z, calculated from the stress free strain and as measured by X-ray reflectivity.

also assume that the Poisson's ratio (ν) follows a rule of mixtures relationship, based on the volume fraction of water, using values of 0.42 and 0.5 for dry Nafion and water, respectively.[17,40] Again, the water volume fraction was determined as a function of relative humidity using a quartz crystal microbalance (Figure S2). Over the humidity range examined (0% to 82%), ν varies from approximately 0.42 to 0.44 (Figure S3). Using these values, we have estimated the swelling strain in the z-direction (ε_z) from the stress free strain, using the expression

$$\varepsilon_z = \varepsilon_o\frac{1+\nu}{1-\nu} \tag{14}$$

which can be derived from eqs 5−8. These calculated values are compared to the z-strain as measured by X-ray reflectivity (Figure 5). The measured values for ε_z are comparable to those calculated from eq 14 over a wide range of relative humidity. These results indicate that our mechanical model, to a first approximation, reflects the swelling strain that develops in the cantilever-supported membrane and that we have reasonable values for ε_o and ν as a function of humidity.

With independent measurements of ΔF_c, ε_o, and ε_z, and knowing the initial dry film thickness of the Nafion on the gold cantilever (216 ± 34 nm), we rearrange eq 11 to calculate the modulus of the thin Nafion film,

$$E = -\frac{\Delta F_c(1-\nu)^2}{h_o[\varepsilon_o^2(1+\nu) + \varepsilon_o(1-\nu)]} \tag{15}$$

The results are shown in Figure 6a, along with literature values for the modulus of bulk Nafion films, over a humidity range of 0% to 100% RH. The modulus decreases with increasing relative humidity, which is to be expected. Considering the approximations made in the humidity-dependent properties (ΔF_c, ε_o, ν, and ε_z) and the scarcity of data at low relative humidity values, the modulus values shown in Figure 6a should be considered an approximation. We are

DOI: 10.1021/acsami.5b04080
ACS Appl. Mater. Interfaces 2015, 7, 17874−17883

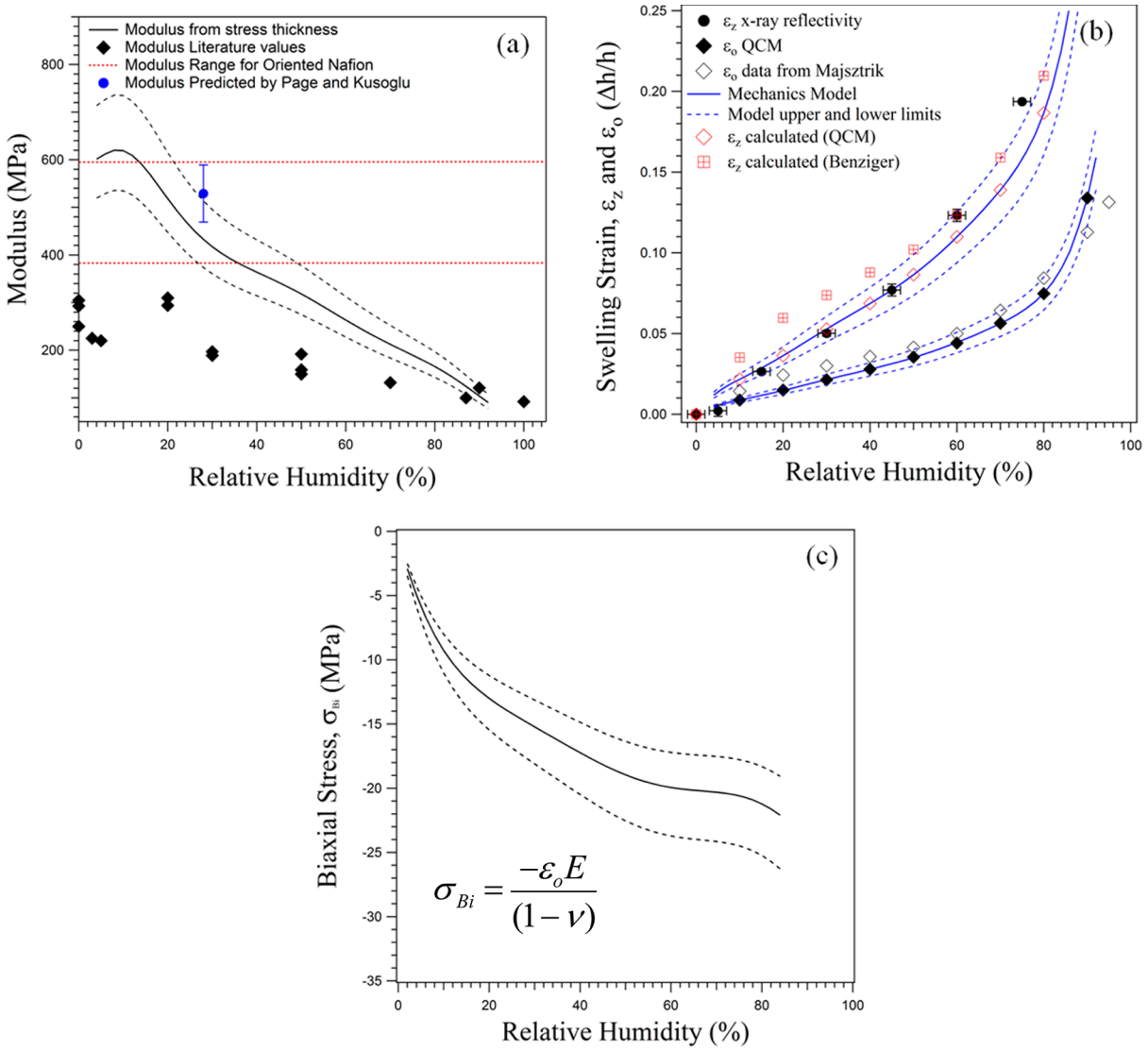

Figure 6. (a) The solid black line represents the modulus values calculated using eq 15 with the dashed lines representing the uncertainty in the dry film thickness, h_o. The red, dotted lines are the range of values for the modulus of Nafion oriented to various degrees,[41,42] and the black diamonds are literature values of the modulus of unoriented Nafion at various relative humidity values.[2,6,9,10,16,17,43−45] The modulus value (blue ●) of a oriented Nafion thin film (ca. 200 nm), as predicted by our recent model,[28] is also shown. (b) The solid blue lines represent the current mechanical model compared to the stress free strain, ε_o, used to calculate the modulus values along with the literature values. The swelling strain, ε_z, is also determined from the modulus values and is compared to that measured by X-ray reflectivity. The predicted ε_z is in good agreement with the X-ray data. (c) The biaxial stress, σ_{Bi}, determined from the wafer curvature method. The dashed lines represent the error in the calculations due to the uncertainty in the dry film thickness.

currently working to improve the model and the measurements in order to provide a more accurate and precise value for the modulus. It is also apparent that our estimated values of the modulus, at low relative humidity, are considerably higher than those reported for bulk Nafion. We have also used the above mechanical model, assuming the literature modulus values for bulk Nafion as a function of RH, in order to calculate both ε_o and ε_z. We were unable to match the model to the data of ε_o and ε_z obtained from our QCM and XR results. In fact, the lower modulus values found in the literature in combination with our stress-thickness measurements resulted in considerably higher strain values compared to our experimental results. This test validated the high modulus values estimated by our model. The literature, combined with GISAXS (see discussion below), was able to reveal, in part, the origin of this increase in apparent modulus. Researchers have shown that Nafion, when oriented, can exhibit a significantly higher tensile and bending modulus when compared to isotropic membranes,[41,42] while the water uptake is largely unaffected. The range of modulus values for oriented Nafion is shown as red horizontal lines in Figure 6a. The Teflon-like backbone of Nafion has an inherently high modulus, and alignment of the chains results in a higher observed modulus. From our earlier work and that of others, it has been demonstrated that unannealed thin films of Nafion on various substrates show a remarkable degree of orientation of both ionic domains and chain segments parallel to the substrate.[18,20,21,26,46] Figure 6b demonstrates the excellent agreement our model has to the measured/calculated values of ε_o and ε_z despite the fact that we do not consider the anisotropic morphology. We are currently modifying our model to account for anisotropy in mechanical properties in addition to removing the anisotropy through high-

DOI: 10.1021/acsami.5b04080
ACS Appl. Mater. Interfaces 2015, 7, 17874−17883

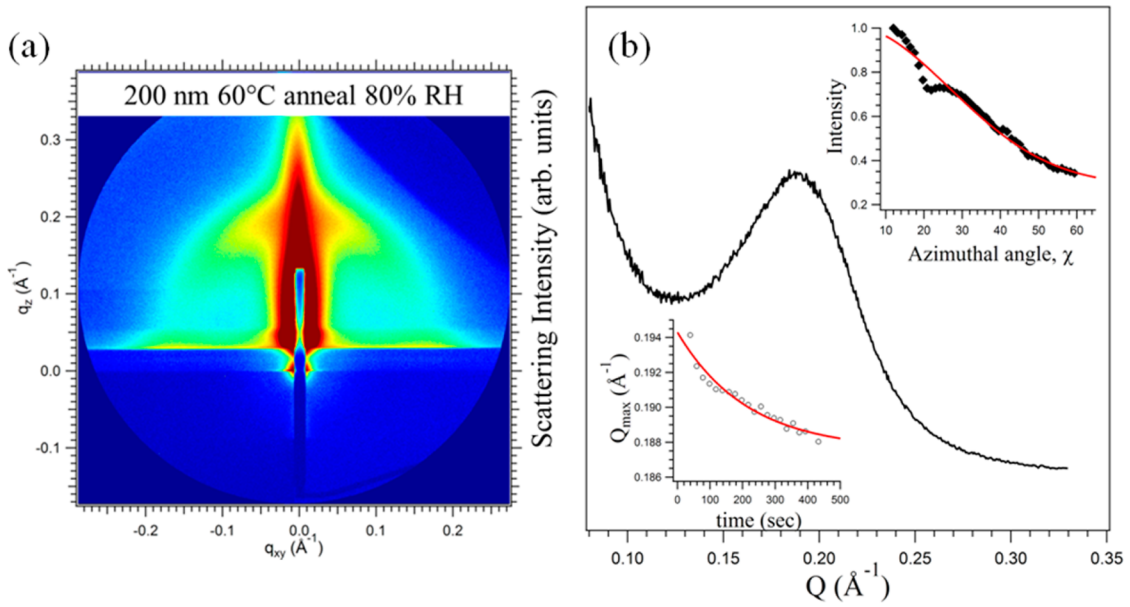

Figure 7. (a) The GISAXS scattering image along with (b) the intensity versus Q as determined from a radial integration of the scattering intensity for a Nafion film (≈200 nm) equilibrated at 80% RH. The peak at approximately 0.19 Å^{-1} is indicative of the correlations between the ionic domains. The upper right inset shows the scattering intensity of the ionomer peak as a function of the azimuthal angle, χ. The χ-dependence clearly demonstrates that the ionic domains are oriented parallel to the substrate. The lower left inset shows the position of the ionomer peak as a function of time after a jump from 0% to 80% RH.

temperature annealing. We also plot in Figure 6c the biaxial stress in the film as a function of relative humidity from the stress-thickness and our estimates of the modulus. As stated earlier, the biaxial stresses experienced by a membrane in a working fuel cell play a major role in the mechanical degradation of the material. Stresses exceeding 20 MPa can be expected for fully constrained and fully hydrated Nafion.[2,9,10] This is consistent with theoretical predictions of dilatational stresses for comparable water vapor activities and degree of constraint.[6,7,10] These data are also consistent with reported literature values for the stresses experienced by membranes clamped in a working PEM fuel cell and demonstrate the ability and comparability of this measurement method to study the hydro-mechanical behavior of membrane materials under humidity cycling.

We have performed in situ GISAXS/GIWAXD on a thin film (ca. 200 nm) spin coated onto a gold substrate (Figure 7). In order to simulate the wafer curvature experiment, the sample was placed in a humidity-controlled chamber and a jump from 0% to 80% RH was performed. During this time, the scattering pattern was collected at fixed time intervals on a CCD detector with an incoming beam at an incident angle of approximately 0.12°. The details of this measurement can be found in an earlier publication.[21] The scattering pattern at equilibrium swelling (80% RH) and analysis is shown in Figure 7. The peak in the 2D scattering pattern at approximately 0.2 Å^{-1} is attributed to the size and spatial distribution of the ionic domains of Nafion, and it is clear from the anisotropic nature of the scattering intensity that the ionic domains are oriented parallel to the substrate surface. This is more apparent in the radially and azimuthally integrated intensity profiles in Figure 7b. The maximum in the peak intensity is related to a distance between ionic domains of about 3 nm. The inset in the upper right-hand corner is the scattering intensity in the azimuthal direction, χ. For an isotropic distribution of the ionic domains, the intensity should be χ-independent and these data clearly indicate that there is an anisotropic distribution of the scattering intensity about the azimuth. Therefore, the Nafion is undoubtedly oriented parallel to the cantilever surface. It should be noted, however, that the in-plane structure is likely to be isotropic due to the coating process. The results of this analysis are consistent with that found in the literature for Nafion thin films, a more detailed description of which can be found in the literature.[18,21−23,26,28] Nafion orientation could explain the high modulus values obtained by cantilever curvature. As previously mentioned, the model used here does not consider anisotropy in the mechanical properties and may explain why the swelling strains cannot be matched perfectly, but it is, to a first approximation, a reasonable model. The water uptake and stress free strain measured in this study are comparable to that for bulk, isotropic membranes. The material is likely to experience a combination of effects which lead to the observed increase in modulus. First, there is the effect of orientation, which has been demonstrated here. Structure−property models that attempt to account for anisotropy in the film morphology clearly demonstrate the importance of orientation.[40] Second, it is possible that the material experiences molecular confinement in the z-direction due to the length-scale of the film thickness. It is not uncommon for polymers to exhibit drastic changes in material properties due to molecular confinement.[18−28] We are currently working to investigate this further with other techniques. For comparison, we have included in Figure 6a the modulus value for a similar thin film at 30% RH obtained using a film buckling technique developed in our laboratory.[28] It is apparent that our estimated modulus from the wafer curvature method yields reasonable values capable of being reproduced by other methods. In future work, we will develop these models further and explore the effect of film thickness and annealing to determine the roles that orientation and molecular confinement have on the mechanical properties of these materials.

DOI: 10.1021/acsami.5b04080
ACS Appl. Mater. Interfaces 2015, 7, 17874−17883

CONCLUSIONS

The biaxial stress and mechanical response of a ≈200 nm Nafion film was measured using a cantilever bending apparatus in conjunction with swelling strain measurements using quartz crystal microbalance and X-ray reflectivity. Specifically, it was demonstrated that the Young's modulus of a Nafion film was two times larger than the modulus values observed for bulk Nafion membranes and decreased with increasing wate activity. The enhancement in modulus of thin Nafion films was attributed to anisotropic orientation of the ionic domains within the film, which was confirmed using grazing incidence small-angle X-ray scattering. The cantilever curvature technique provided a means to measure the swelling induced stresses during hydration cycles. It was observed that in a ≈200 nm Nafion film the average biaxial stress can exceed 20 MPa as the humidity approaches 80% RH. This study demonstrates a cantilever bending platform that can measure the swelling induced biaxial stress similar to those experienced in a working hydrogen fuel cell and can easily be expanded to incorporate novel PEM materials.

ASSOCIATED CONTENT

Supporting Information

The Supporting Information is available free of charge on the ACS Publications website at DOI: 10.1021/acsami.5b04080.

Humidity sensor calibration; water update determination via quartz crystal microbalance (QCM); method used for estimating Poisson's ratio in the swollen Nafion film (PDF)

AUTHOR INFORMATION

Corresponding Author

*E-mail: gery.stafford@nist.gov.

Notes

The authors declare no competing financial interest.

ACKNOWLEDGMENTS

The authors gratefully acknowledge Carlos Beauchamp, Bradley Frieberg, Christopher Stafford, and Christopher L. Soles of NIST for technical contributions, programmatic support, and several lively scientific discussions. S.A.E. and B.W.R. acknowledge support from the NIST NRC Fellowship program. Certain commercial equipment, instruments, or materials are identified in this paper in order to specify the experimental procedure adequately. Such identification is not intended to imply recommendation or endorsement by the National Institute of Standards and Technology, nor is it intended to imply that the materials or equipment identified are necessarily the best available for the purpose. Research used resources of the Center for Functional Nanomaterials, and the National Synchrotron Light Source, which are U.S. DOE Office of Science Facilities, at Brookhaven National Laboratory under Contract No. DE-SC0012704.

REFERENCES

(1) Mauritz, K.; Moore, R. State of Understanding of Nafion. *Chem. Rev.* **2004**, *104*, 4535−85.

(2) Kusoglu, A.; Tang, Y.; Lugo, M.; Karlsson, A. M.; Santare, M. H.; Cleghorn, S.; Johnson, W. B. Constitutive Response and Mechanical Properties of PFSA Membranes in Liquid Water. *J. Power Sources* **2010**, *195*, 483.

(3) Lai, Y.-H.; Mittelsteadt, C. K.; Gittleman, C. S.; Dillard, D. A. Viscoelastic Stress Model and Mechanical Charaterization of Perfluorosulfonic Acid (PFSA) Polymer Electrolyte Membranes, *Third International Conference on Fuel Cell Science, Engineering and Technology*, May 23−25, 2005, Ypsilanti, Michigan; DOI: 10.1115/FUELCELL2005-74120.

(4) Lai, Y.-H.; Mittelsteadt, C. K.; Gittleman, C. S.; Dillard, D. A. Viscoelastic Stress Analysis of Constrained Proton Exchange Membranes Under Humidity Cycling. *J. Fuel Cell Sci. Technol.* **2009**, *6*, 021002−1.

(5) Majsztrik, P.; Bocarsly, A.; Benziger, J. Water Permeation through Nafion membranes: The role of water activity. *J. Phys. Chem. B* **2008**, *112*, 16280.

(6) Tang, Y.; Santare, M. H.; Karlsson, A. M.; Cleghorn, S.; Johnson, W. B. Stresses in Proton Exchange Membranes Due to Hygro-Thermal Loading. *J. Fuel Cell Sci. Technol.* **2006**, *3*, 119.

(7) Weber, A. Z.; Newman, J. A. Theoretical Study of Membrane Constraint in Polymer-Electrolyte Fuel Cells. *AIChE J.* **2004**, *50*, 3215.

(8) Huang, X.; Solasi, R.; Zou, Y.; Feshler, M.; Reifsnider, K.; Condit, D.; Burlatsky, S.; Madden, T. Mechanical Endurance of Polymer Electrolyte Membrane and PEM Fuel Cell Durability. *J. Polym. Sci., Part B: Polym. Phys.* **2006**, *44*, 2346.

(9) Kusoglu, A.; Karlsson, A. M.; Santare, M. H.; Cleghorn, S.; Johnson, W. B. Mechanical Behavior of Fuel Cell Membranes Under Humidity Cycles and Effect of Swelling Anisotropy on the Fatigue Stresses. *J. Power Sources* **2007**, *170*, 345.

(10) Kusoglu, A.; Karlsson, A. M.; Santare, M. H.; Cleghorn, S.; Johnson, W. B. Mechanical Response of Fuel Cell Membranes Subjected to a Hygro-Thermal Cycle. *J. Power Sources* **2006**, *161*, 987.

(11) Solasi, R.; Zou, Y.; Huang, X.; Reifsnider, K.; Condit, D. On Mechanical Behavior and in-Plane Modeling of Constrained PEM Fuel Cell Membranes Subjected to Hydration and Temperature Cycles. *J. Power Sources* **2007**, *167*, 366.

(12) Silberstein, M. N.; Boyce, M. C. Hygro-Thermal Mechanical Behavior of Nafion During Constrained Swelling. *J. Power Sources* **2011**, *196*, 3452.

(13) Silberstein, M. N.; Pillai, P. V.; Boyce, M. C. Biaxial Elastic-Viscoplastic Behavior of Nafion Membranes. *Polymer* **2011**, *52*, 529.

(14) Solasi, R.; Zou, Y.; Huang, X. Y.; Reifsnider, K. A Time and Hydration Dependent Viscoplastic Model for Polyelectrolyte Membranes in Fuel Cells. *Mech. Time-Depend. Mater.* **2008**, *12*, 15.

(15) Yoon, W.; Huang, X. A Multiphysics Model of PEM Fuel Cell Incorporating the Cell Compression Effects. *J. Electrochem. Soc.* **2010**, *157*, B680.

(16) Satterfield, M. B.; Majsztrik, P. W.; Ota, H.; Benziger, J. B.; Bocarsly, A. B. Mechanical Properties of Nafion and Titania/Nafion Composite Membranes for Polymer Electrolyte Membrane Fuel Cells. *J. Polym. Sci., Part B: Polym. Phys.* **2006**, *44*, 2327.

(17) Kusoglu, A.; Tang, Y. L.; Santare, M. H.; Karlsson, A. M.; Cleghorn, S.; Johnson, W. B. Stress-Strain Behavior of Perfluorosulfonic Acid Membranes at Various Temperatures and Humidities: Experiments and Phenomenological Modeling. *J. Fuel Cell Sci. Technol.* **2009**, *6* (1), 011012−8.

(18) Bass, M.; Berman, A.; Singh, A.; Konovalov, O.; Freger, V. Surface-Induced Micelle Orientation in Nafion Films. *Macromolecules* **2011**, *44* (8), 2893−2899.

(19) Dishari, S. K.; Hickner, M. A. Antiplasticization and Water Uptake of Nafion Thin Films. *ACS Macro Lett.* **2012**, *1* (2), 291−295.

(20) Dura, J. A.; Murthi, V. S.; Hartman, M.; Satija, S. K.; Majkrzak, C. F. Multilamellar Interface Structures in Nafion. *Macromolecules* **2009**, *42* (13), 4769−4774.

(21) Eastman, S. A.; Kim, S.; Page, K. A.; Rowe, B. W.; Kang, S.; Soles, C. L.; Yager, K. G. Effect of Confinement on Structure, Water Solubility, and Water Transport in Nafion Thin Films. *Macromolecules* **2012**, *45* (19), 7920−7930.

(22) Modestino, M. A.; Kusoglu, A.; Hexemer, A.; Weber, A. Z.; Segalman, R. A. Controlling Nafion Structure and Properties via Wetting Interactions. *Macromolecules* **2012**, *45* (11), 4681−4688.

DOI: 10.1021/acsami.5b04080
ACS Appl. Mater. Interfaces 2015, 7, 17874−17883

(23) Modestino, M. A.; Paul, D. K.; Dishari, S.; Petrina, S. A.; Allen, F. I.; Hickner, M. A.; Karan, K.; Segalman, R. A.; Weber, A. Z. Self-Assembly and Transport Limitations in Confined Nafion Films. *Macromolecules* **2013**, *46* (3), 867−873.
(24) Paul, D. K.; Fraser, A.; Karan, K. Towards the Understanding of Proton Conduction Mechanism in PEMFC Catalyst Layer: Conductivity of Adsorbed Nafion Films. *Electrochem. Commun.* **2011**, *13* (8), 774−777.
(25) Siroma, Z.; Kakitsubo, R.; Fujiwara, N.; Ioroi, T.; Yamazaki, S. I.; Yasuda, K. Depression of Proton Conductivity in Recast Nafion (R) Film Measured on Flat Substrate. *J. Power Sources* **2009**, *189* (2), 994−998.
(26) Kusoglu, A.; Kushner, D.; Paul, D. K.; Karan, K.; Hickner, M. A.; Weber, A. Z. Impact of Substrate and Processing on Confinement of Nafion Thin Films. *Adv. Funct. Mater.* **2014**, *24* (30), 4763−4774.
(27) Paul, D. K.; Karan, K.; Docoslis, A.; Giorgi, J. B.; Pearce, J. Characteristics of Self-Assembled Ultrathin Nafion Films. *Macromolecules* **2013**, *46* (9), 3461−3475.
(28) Page, K. A.; Kusoglu, A.; Stafford, C. M.; Kim, S.; Kline, R. J.; Weber, A. Z. Confinement-Driven Increase in Ionomer Thin-Film Modulus. *Nano Lett.* **2014**, *14*, 2299.
(29) Stafford, C. M.; Roskov, K. E.; Epps, T. H., III; Fasolka, M. J. Generating Thickness Greadients of Thin Polymer Films via Flow Coating. *Rev. Sci. Instrum.* **2006**, *77*, 023908.
(30) Stoney, G. G. The Tension of Metallic Films Deposited by Electrolysis. *Proc. R. Soc. London, Ser. A* **1909**, *82* (553), 172−175.
(31) Kongstein, O. E.; Bertocci, U.; Stafford, G. R. In Situ Stress Measurements During Copper Electrodeposition on (111)-Textured Au. *J. Electrochem. Soc.* **2005**, *152*, C116.
(32) Stafford, G. R.; Bertocci, U. In Situ Stress and Nanogravimetric Measurements during Underpotential Deposition of Bismuth on (111)-Textured Au. *J. Phys. Chem. B* **2006**, *110*, 15493.
(33) Parratt, L. G. Surface Studies of Solids by Total Reflection of X-rays. *Phys. Rev.* **1954**, *95* (2), 359−369.
(34) Li, Y.; Dillard, D. A.; Lai, Y.-H.; Case, S. W.; Ellis, M. W.; Budinski, M. K.; Gittleman, C. S. Experimental Measurement of Stress and Strain in Nafion Membrane during Hydration Cycles. *J. Electrochem. Soc.* **2012**, *159*, B173.
(35) Bauer, F.; Denneler, S.; Willert-Porada, M. Influence of Temperature and Humidity on the Mechanical Properties of Nafion®117 Polymer Electrolyte Membrane. *J. Polym. Sci., Part B: Polym. Phys.* **2005**, *43*, 786.
(36) Majsztrik, P. W.; Bocarsly, A. B.; Benziger, J. B. Viscoelastic Response of Nafion. Effects of Temperature and Hydration on Tensile Creep. *Macromolecules* **2008**, *41*, 9849.
(37) Choi, P.; Datta, R. Sorption in Proton-Exchange Membranes. An Explanation of Schroeder's Paradox. *J. Electrochem. Soc.* **2003**, *150*, E601.
(38) Boettinger, W. J.; Johnson, C. E.; Bendersky, L. A.; Moon, K.-W.; Williams, M. E.; Stafford, G. R. Whisker and Hillock Formation on Sn, Sn−Cu and Sn−Pb Electrodeposits. *Acta Mater.* **2005**, *53*, 5033−5050.
(39) Zawodzinski, T. A.; Springer, T. E.; Davey, J.; Jestel, R.; Lopez, C.; Valerio, J.; Gottesfeld, S. A Comparative-Study of Water-Uptake by and Transport through Ionomeric Fuel-Cell Membranes. *J. Electrochem. Soc.* **1993**, *140* (7), 1981−1985.
(40) Kusoglu, A.; Karlsson, A. M.; Santare, M. H. Structure-Property Relationship in Ionomer Membranes. *Polymer* **2010**, *51* (6), 1457−1464.
(41) Lin, J.; Wu, P. H.; Wycisk, R.; Pintauro, P. N.; Shi, Z. Q. Properties of Water in Prestretched Recast Nafion. *Macromolecules* **2008**, *41* (12), 4284−4289.
(42) Lin, J.; Wu, P.-H.; Wycisk, R.; Pintauro, P. PEM Fuel Cell Properties of Pre-Stretched Recast Nafion®. *ECS Trans.* **2008**, *16* (2), 1195−1204.
(43) Ballengee, J. B.; Pintauro, P. N. Composite Fuel Cell Membranes from Dual-Nanofiber Electrospun Mats. *Macromolecules* **2011**, *44* (18), 7307−7314.
(44) Choi, P.; Jalani, N. H.; Thampan, T. M.; Datta, R. Consideration of Thermodynamic, Transport, and Mechanical Properties in the Design of Polymer Electrolyte Membranes for Higher Temperature Fuel Cell Operation. *J. Polym. Sci., Part B: Polym. Phys.* **2006**, *44* (16), 2183−2200.
(45) Tang, Y. L.; Karlsson, A. M.; Santare, M. H.; Gilbert, M.; Cleghorn, S.; Johnson, W. B. An Experimental Investigation of Humidity and Temperature Effects on the Mechanical Properties of Perfluorosulfonic Acid Membrane. *Mater. Sci. Eng., A* **2006**, *425* (1−2), 297−304.
(46) Kim, S.; Dura, J. A.; Page, K. A.; Rowe, B. W.; Yager, K. G.; Lee, H.; Soles, C. L. Surface-induced Nanostructure and Water Transport of Thin Proton-Conducting Polymer Films. *Macromolecules* **2013**, *46*, 5630−5637.

DOI: 10.1021/acsami.5b04080
ACS Appl. Mater. Interfaces 2015, 7, 17874−17883